

Original articles

Interface spaces for the Multiscale Robin Coupled Method in reservoir simulation

Rafael T. Guiraldello^a, Roberto F. Ausas^a, Fabricio S. Sousa^a, Felipe Pereira^b,
Gustavo C. Buscaglia^{a,*}

^a Instituto de Ciências Matemáticas e de Computação, Universidade de São Paulo, Av. Trabalhador São-carlense, 400, 13566-590, São Carlos, SP, Brazil

^b Department of Mathematical Sciences, The University of Texas at Dallas, 800 W. Campbell Road, Richardson, Texas 75080-3021, USA

Received 26 January 2018; received in revised form 27 June 2018; accepted 3 September 2018

Available online 24 November 2018

Abstract

The Multiscale Robin Coupled Method (MRCM) is a recent multiscale numerical method based on a non-overlapping domain decomposition procedure. One of its hallmarks is that the MRCM allows for the independent definition of interface spaces for pressure and flux over the skeleton of the decomposition. The accuracy of the MRCM depends on the choice of these interface spaces, as well as on an algorithmic parameter β in the Robin interface conditions imposed at the subdomain boundaries. This work presents an extensive numerical assessment of the MRCM in both of these aspects. Two types of interface spaces are implemented: usual piecewise polynomial spaces and informed spaces, the latter obtained from sets of snapshots by dimensionality reduction. Different distributions of the unknowns between pressure and flux are explored. Two non-dimensionalizations of β are tested. The assessment is conducted on realistic, high contrast, channelized permeability fields from a SPE benchmark database. The results show that β , suitably non-dimensionalized, can be fixed to unity to avoid any indeterminacy in the method. Further, with both types of spaces it is observed that a balanced distribution of the interface unknowns between pressure and flux renders the MRCM quite attractive both in accuracy and in computational cost, competitive with other multiscale methods from the literature
© 2018 International Association for Mathematics and Computers in Simulation (IMACS). Published by Elsevier B.V. All rights reserved.

Keywords: Porous media; Darcy flow; Domain decomposition; Multiscale approximation; Robin boundary conditions; Optimized Schwarz; Two-Lagrange-multiplier method; Reservoir simulation

1. Introduction

Multiscale domain decomposition methods have received considerable attention from the scientific community due to their potential to solve efficiently elliptic problems with rapidly varying coefficients in parallel multi-core computers. This class of methods approximates the exact solution by solving uncoupled local problems on non-overlapping subdomains, along with one *global* problem (or *interface* problem) associated with the coupling between subdomains through their boundaries. In fact, consistency conditions require the imposition of some form of continuity

* Corresponding author at: Instituto de Ciências Matemáticas e de Computação, Universidade de São Paulo, Av. Trabalhador São-carlense, 400, 13566-590, São Carlos, SP, Brazil.

E-mail addresses: trevi@usp.br (R.T. Guiraldello), rfausas@icmc.usp.br (R.F. Ausas), fsimeoni@icmc.usp.br (F.S. Sousa), luisfelipe.pereira@utdallas.edu (F. Pereira), gustavo.buscaglia@icmc.usp.br (G.C. Buscaglia).

<https://doi.org/10.1016/j.matcom.2018.09.027>

0378-4754/© 2018 International Association for Mathematics and Computers in Simulation (IMACS). Published by Elsevier B.V. All rights reserved.

of fluxes and of pressures at interfaces between neighbor subdomains. Different methods have been developed based on distinct approaches to address the continuity issue. We mention, for instance, the Multiscale Mortar Mixed Finite Element Method (MMMFEM) [2] and the Multiscale Hybrid-Mixed Method (MHM) [1,17], as some well known procedures of this type. In the MMMFEM, the pressure continuity is weakly satisfied in the fine-grid scale (the scale of the local grid of each subdomain, usually denoted by h), while normal flux continuity is ensured in a much larger scale ($H \gg h$), usually associated with the size of the subdomains. Conversely in the MHM, continuity of the normal fluxes is satisfied at the fine-grid h scale, while pressure continuity is only imposed at the larger H scale.

The design of accurate multiscale domain decomposition methods for channelized, high-contrast porous media, remains as an important challenge because in typical problems posed by the oil industry existing multiscale methods may produce inaccurate numerical approximations [15].

In our search for more accurate procedures, here we investigate an improved version of the recently proposed Multiscale Robin Coupled method (MRCM) [15]. This method is based on the domain decomposition of Douglas et al. [12] and on the Multiscale Mixed Method (MuMM) of Francisco et al. [13], and ensures weak continuity of both normal fluxes and pressures through the imposition of Robin-type boundary conditions, namely

$$-\beta_i \mathbf{u}^i \cdot \check{\mathbf{n}}^i + p^i = \beta_j \mathbf{u}^j \cdot \check{\mathbf{n}}^j + p^j, \quad (1)$$

at the interface Γ_{ij} between subdomains (identified by i and j), usually in a scale that is larger than the fine-grid scale. In Eq. (1) p^i and \mathbf{u}^i are pressure and velocity of subdomain i at the interface, and $\check{\mathbf{n}}^i = -\check{\mathbf{n}}^j$ is the outwards unit normal. The MRCM can be seen as a generalization of the above mentioned methods depending on the parameter β_i : the MMMFEM (respectively, the MHM) is recovered as $\beta_i \rightarrow 0$ (respectively, $\beta_i \rightarrow +\infty$) for all i .

The accuracy and cost of multiscale domain decomposition methods are mainly determined by the choice of the *interface space*, i.e., the space on which the global problem is posed. This space consists of functions defined on the collection of interfaces between subdomains, or *skeleton* of the partition, $\Gamma = \cup_{i \neq j} \Gamma_{ij}$, where Γ_{ij} denotes the interface between nearest-neighbor subdomains. For the MMMFEM the interface space is a **pressure space** \mathcal{P}_H , while for the MHM it is a **flux space** \mathcal{U}_H . A salient feature of the MRCM, with β_i different from 0 and $+\infty$, is that its global interface problem is posed on the direct product $\mathcal{P}_H \times \mathcal{U}_H$ of a pressure space and a flux space, both defined on the skeleton and which can be chosen independently. This allows us to explore an interesting question: Assume that one decides to allocate k unknowns at each interface Γ_{ij} of the skeleton. How does their distribution between pressure unknowns and flux unknowns affect the accuracy and cost-effectiveness of the method?

Of course the approximation capabilities of the interface space depends not just on its dimension (i.e., number of unknowns) but also on the functions it consists of. The first reported implementations of MMMFEM, MHM and MRCM adopted piecewise polynomial spaces over the interfaces, which are the simplest to code and analyze. It is however accepted nowadays that polynomial spaces are not optimal for highly heterogeneous problems, and different kinds of problem-dependent approximation spaces (*informed spaces*, in short) have been proposed for multiscale finite element [3,8] and finite volume [18] methods. The latter was extended to several nonlinear complex cases, including the compressible and compositional cases as well as fractures [4,11,19,20]. The combination of informed spaces with the MMMFEM has recently been studied by Chung et al. [10], while it remains unexplored for the MHM. In line with this trend, this work explores a strategy for building informed spaces at the interfaces for the MRCM. In this way, we explore the question of optimal allocation of unknowns between pressure and flux not just with polynomials but also with spaces that are more suitable for highly heterogeneous media. Moreover, once the MHM is a particular case of the MRCM, a first study of combining the MHM with informed spaces is also produced.

Our numerical results indicate that, typically, the optimal accuracy is attained somewhere in between the MMMFEM (all unknowns for pressure) and the MHM (all unknowns for flux). In other words, the solution of minimal error is produced by the MRCM for some specific choice of its algorithmic parameters. Further, it is shown that through appropriate dimensional analysis it is possible to fix all parameters of the MRCM automatically, resulting in a fully-determined method that is competitive with known ones. In particular, it is recommended that the number of unknowns for interface pressure is equal to (or slightly smaller than) the number of unknowns for interface flux. In this way we arrive at a method that is effective for all layers in the SPE10 database. The construction of the informed spaces needs however to be improved, since the method exhibits comparable overall accuracy with polynomial and informed interface spaces. There exist multiscale iterative methods, that include global information on the multiscale basis functions and show improvements in terms of accuracy (see e.g. [9,16]). The development and discussion of such procedures for the MRCM is out of the scope of this article and is left for future work. However, we remark

that informed interface spaces do show improved approximation of fluxes in regions of the domain with high-contrast formations.

The plan of this article is as follows: The MRCM is briefly recalled in Section 2, adopting a fine grid discretization consisting of lowest order Raviart–Thomas finite elements RT_0 and general spaces \mathcal{P}_H and \mathcal{U}_H at the skeleton Γ . The reader should recall that the RT_0 elements are equivalent to the popular cell-centered finite volume method with two-point flux approximation. The strategy adopted for building the interface spaces is described in Section 3. It is similar to strategies proposed by other authors, such as the empirical interpolation technique used by Calo et al. [5,6] in the context of multiscale finite elements. With these elements at hand, Section 4 is then devoted to numerical experiments addressing the questions of selection of optimal algorithmic parameters and of optimal allocation of interface unknowns between pressures and fluxes. The geological data used in the experiments are two-dimensional layers of the SPE10 benchmark database, with different degrees of channelization.

2. The multiscale Robin coupled method

2.1. Discrete variational formulation

Let us consider a fine grid \mathcal{T}_h , i.e., a subdivision of the domain $\Omega \subset \mathbb{R}^d$ consisting of d -dimensional cuboids of size h , and a decomposition of Ω in subdomains $\{\Omega_i\}_{i=1,\dots,m}$, of characteristic size $H \gg h$, such that each element $K \in \mathcal{T}_h$ belongs to one and only one of the subdomains. Moreover, let Γ be the skeleton of the domain decomposition, as the union of all interfaces $\Gamma_{i,j} = \overline{\Omega}_i \cap \overline{\Omega}_j$. The discrete variational formulation of the MRCM is written over the discrete lowest order Raviart–Thomas spaces for velocity and pressure, defined as

$$\mathbf{V}_h^i = \{ \mathbf{v} \in H(\text{div}, \Omega_i), v_j(\mathbf{x})|_K = p_{j1}(x_1)p_{j2}(x_2)\dots, \forall K \in \mathcal{T}_h^i, \text{ with } p_{jk} \in \mathbb{P}_1 \text{ if } j = k, p_{jk} \in \mathbb{P}_0 \text{ if } j \neq k \}, \tag{2}$$

$$\mathbf{V}_{hy}^i = \{ \mathbf{v} \in \mathbf{V}_h^i, \mathbf{v} \cdot \check{\mathbf{n}} = y \text{ on } \partial\Omega_i \cap \partial\Omega_u \}, \tag{3}$$

$$\mathcal{Q}_h^i = \{ q \in L^2(\Omega_i), q(\mathbf{x})|_K \in \mathbb{P}_0 \}, \tag{4}$$

with y being a piecewise constant function defined on the edges of $\partial\Omega_u$ and \mathbb{P}_k the usual space of polynomials of degree up to k .

We denote by \mathcal{E}_h the set of all edges/faces of \mathcal{T}_h in the skeleton Γ . A unique normal $\check{\mathbf{n}}$ is defined as

$$\check{\mathbf{n}}(e) \doteq \text{exterior normal to } \partial\Omega_{\min\{i,j\}}, \text{ if } e \in \Gamma_{i,j} \tag{5}$$

for every e in \mathcal{E}_h . The spaces for pressures and fluxes at subdomain interfaces that will be considered here consist of functions that are constant on each e of \mathcal{E}_h , i.e., they are subsets of

$$F_h(\mathcal{E}_h) = \{ f : \mathcal{E}_h \rightarrow \mathbb{R} \mid f|_e \in \mathbb{P}_0, \forall e \in \mathcal{E}_h \}. \tag{6}$$

To finally state the variational formulation of the MRCM, consider low-dimensional subspaces \mathcal{U}_H and \mathcal{P}_H of $F_h(\mathcal{E}_h)$. The MRCM consists in finding $(\mathbf{u}_h^i, p_h^i) \in \mathbf{V}_{hz}^i \times \mathcal{Q}_h^i$, for $i = 1, \dots, m$, and $(U_H, P_H) \in \mathcal{U}_H \times \mathcal{P}_H$ such that

$$\begin{aligned} (K^{-1}\mathbf{u}_h^i, \mathbf{v})_{\Omega_i} - (p_h^i, \nabla \cdot \mathbf{v})_{\Omega_i} \\ + (P_H - \beta_i U_H \check{\mathbf{n}}^i \cdot \check{\mathbf{n}} + \beta_i \mathbf{u}_h^i \cdot \check{\mathbf{n}}^i, \mathbf{v} \cdot \check{\mathbf{n}}^i)_{\partial\Omega_i \cap \Gamma} = - (g, \mathbf{v} \cdot \check{\mathbf{n}}^i)_{\partial\Omega_i \cap \partial\Omega_p} \end{aligned} \tag{7}$$

$$(q, \nabla \cdot \mathbf{u}_h^i)_{\Omega_i} = (f, q)_{\Omega_i} \tag{8}$$

$$\sum_{i=1}^m (\mathbf{u}_h^i \cdot \check{\mathbf{n}}^i, M_H)_{\partial\Omega_i \cap \Gamma} = 0 \tag{9}$$

$$\sum_{i=1}^m (\beta_i (\mathbf{u}_h^i \cdot \check{\mathbf{n}}^i - U_H \check{\mathbf{n}}^i \cdot \check{\mathbf{n}}), V_H \check{\mathbf{n}}^i \cdot \check{\mathbf{n}})_{\partial\Omega_i \cap \Gamma} = 0 \tag{10}$$

hold for all $(\mathbf{v}, q) \in \mathbf{V}_{h0}^i \times \mathcal{Q}_h^i, \forall i = 1, \dots, m$, for all $M_H \in \mathcal{P}_H$ and for all $V_H \in \mathcal{U}_H$. Above, the symbol $(\cdot, \cdot)_A$ denotes the scalar product of $L^2(A)$.

The existence and uniqueness of the solution of this variational formulation is proved in [15]. It only requires that

$$\sum_{i=1}^m (\beta_i V_H, V_H) > 0, \quad \forall V_H \in \mathcal{U}_H, \quad V_H \neq 0. \quad (11)$$

This condition is easy to check, since

$$\sum_{i=1}^m (\beta_i V_H, V_H) = \sum_{i=1}^m \int_{\partial\Omega_i \cap \Gamma} \beta_i V_H^2 = \int_{\Gamma} (\beta^+ + \beta^-) V_H^2, \quad (12)$$

where the plus and minus superscript refer to the two sides of Γ . If the functions β_i , assumed non-negative, are not identically zero on both sides of Γ and on the whole support of some V_H , then the solution is unique. In the extreme case that all β_i 's are identically zero, then \mathcal{U}_H must be zero for the problem to be well-posed. This reduces the formulation to the MMMFEM.

Remark 1. Actually, the variational formulation also holds without the conditions $\mathcal{P}_H \subset F_h(\mathcal{E}_h)$, $\mathcal{U}_H \subset F_h(\mathcal{E}_h)$. The necessary and sufficient conditions are, in fact, (11) together with the same inf–sup compatibility of the MMMFEM, namely that for each nonzero $M_H \in \mathcal{P}_H$ there exists i ($1 \leq i \leq m$) such that

$$\sup_{\mathbf{v} \in \mathbf{V}_{h0}^i} (\mathbf{v} \cdot \mathbf{n}^i, M_H)_{\partial\Omega_i \cap \Gamma} > 0 \quad (13)$$

For the case of the RT₀ velocity approximation, this is equivalent to

$$\sup_{A_h \in F_h(\mathcal{E}_h)} (A_h, M_H)_{\Gamma} > 0,$$

which is automatically satisfied if $\mathcal{P}_H \subset F_h(\mathcal{E}_h)$. Otherwise condition (13) must be checked independently.

The implementation performed here strictly follows the one presented in [15], sharing similarities with the works of Ganis & Yotov [14] and Francisco et al. [13]. Note that the linear system associated with Eqs. (7)–(10) is of a size comparable to that of the original, undecomposed problem. However, the solution to the problem written in terms of Eqs. (7)–(10) can be, locally, expressed in terms of linear combinations of multiscale basis functions. The construction of such basis functions is naturally parallelizable.

By assuming that the interface variables (U_H, P_H) are known, one can uncouple Eqs. (7)–(8) from Eqs. (9)–(10). The first set of equations will produce local problems for the computation of the multiscale basis functions. The set of multiscale basis functions is then used on Eqs. (9)–(10) to generate a global linear system to be solved for the interface variables, coupling the local solutions while ensuring the compatibility conditions between subdomains. The final solution is then obtained by linear combination of the previously computed multiscale basis functions. The interested reader is referred to Guiraldello et al. [15] for a thorough explanation of the implementation of this numerical scheme.

3. Interface spaces: Polynomial and informed

The original implementation of the MRCM used piecewise polynomial spaces over the skeleton Γ of the domain decomposition, both for pressure \mathcal{P}_H and flux \mathcal{U}_H . More precisely, we have considered spaces made up of the elementwise constant fine grid representation of polynomials over the interface elements

$$\mathcal{U}_H = \mathcal{U}_H^{\text{pol}, \ell_U + 1} = \{V_H, V_H|_e = \Pi_0(q), q \in \mathbb{P}_{\ell_U}(e), e \in \mathcal{T}_H\}, \quad (14)$$

$$\mathcal{P}_H = \mathcal{P}_H^{\text{pol}, \ell_P + 1} = \{M_H, M_H|_e = \Pi_0(q), q \in \mathbb{P}_{\ell_P}(e), e \in \mathcal{T}_H\}, \quad (15)$$

where \mathbb{P}_k , $k = \ell_U$ or ℓ_P , is the space of polynomials of degree $\leq k$ and Π_0 is the L^2 -projection of a function of $\mathbb{P}_k(e)$ onto the space $F_h(e)$, $e \in \mathcal{T}_H$. The superscript added to the symbol for each space contains the class of functions adopted (“pol” for polynomials, “inf” for informed) followed by the number of degrees of freedom on each edge of \mathcal{T}_H . Notice that \mathcal{U}_H and \mathcal{P}_H are defined independently at each edge (face in 3D), with no continuity at corner points.

One alternative to polynomial spaces is, as previously mentioned, informed spaces, whose construction is a two-step process: (i) construction of the so called *snapshot space* by solving local problems on regions containing the interfaces $\Gamma_{i,j}$ of the domain decomposition (i.e., oversampling) and considering some parameterization (for example, on the boundary conditions of these local problems) and (ii) selection of the final *informed space* by applying a

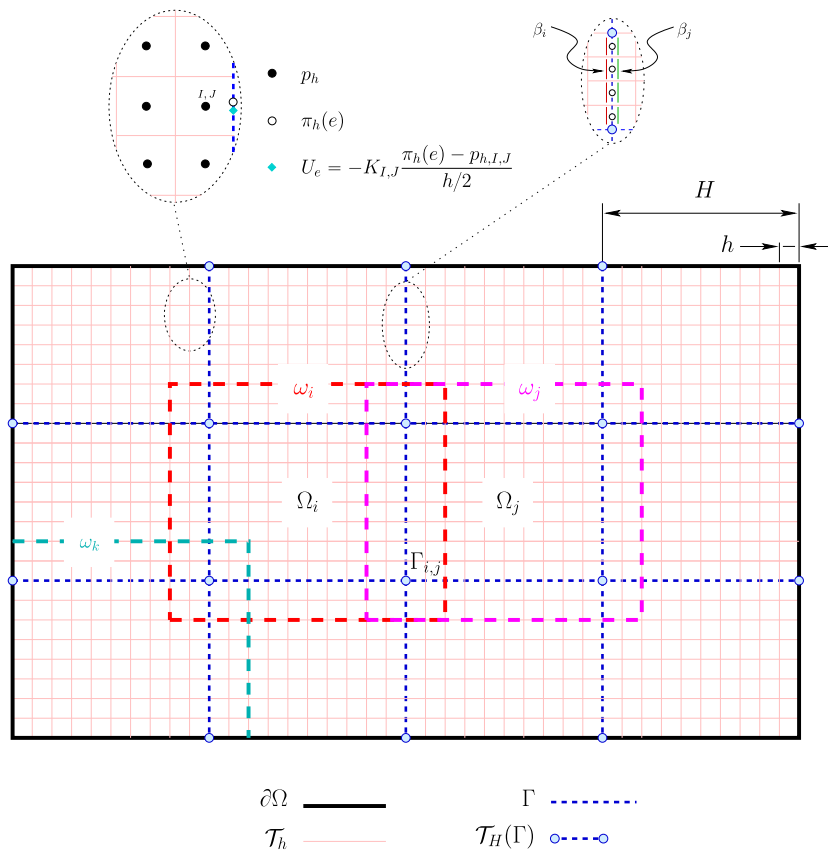


Fig. 1. Computational domain decomposition and oversampling regions.

dimensionality reduction technique (SVD, POD, etc.) to end up with a coarsened interface problem of affordable size and whose solution approximates well the fine grid solution.

By oversampling, we associate to each subdomain Ω_k a new region ω_k that contains it. Fig. 1 shows a few examples of the oversampling regions ω_k for an interior subdomain and for a subdomain that intersects the boundary of Ω . This way, the ω_k 's clearly contain the whole of $\partial\Omega_k \cap \Gamma$. This decomposition essentially follows the original domain decomposition of Ω by slightly augmenting the size of the local problems by just a few layers of fine grid cells that are now shared by several processes. This is expected to be efficient in terms of message passing and avoids dealing with more than one decomposition of Ω . Although in the linear case this would not be a serious drawback since this stage of the computation is done *offline*, in the non-linear case periodic recomputation of the basis functions is needed and switching dynamically between very distinct domain decompositions would lead to an undesirable computational burden.

Consider interface $\Gamma_{i,j}$ and corresponding subdomains ω_k , $k = i, j$. Their boundaries are formed by a collection of fine grid faces $e_m \in \mathcal{T}_h$, $m = 1, 2, \dots, N_k$. In order to build the snapshot space for interface $\Gamma_{i,j}$ we solve N_K local Darcy problems on each oversampling region ω_k ($k = i, j$), i.e.,

$$\begin{aligned}
 \mathbf{u}_h^{k,m} &= -K \nabla p_h^{k,m} && \text{in } \omega_k \\
 \nabla \cdot \mathbf{u}_h^{k,m} &= C_{k,m} && \text{in } \omega_k \\
 \mathcal{B}(\mathbf{u}_h^{k,m}, p_h^{k,m}) &= \delta_m(x) && \text{on } \partial\omega_k
 \end{aligned} \tag{16}$$

The function $\delta_m(x)$ takes the value 1 if $x \in e_m$ and 0 otherwise. In (16), \mathcal{B} is a boundary operator which enforces either pressure boundary conditions on $\partial\omega_k$, i.e.,

$$\mathcal{B}(\mathbf{u}_h^{k,m}, p_h^{k,m}) = p_h^{k,m} \tag{17}$$

in which case the source term $C_{k,m}$ is identically equal to zero, or flux boundary conditions on $\partial\omega_k$, i.e.,

$$\mathcal{B}(\mathbf{u}_h^{k,m}, p_h^{k,m}) = \mathbf{u}_h^{k,m} \cdot \check{\mathbf{n}}_{\partial\omega_k} \tag{18}$$

and the source term $C_{k,m}$ satisfies the compatibility condition

$$\int_{\omega_k} C_{k,m} = \int_{\partial\omega_k} \delta_m. \tag{19}$$

After solving these problems, we retrieve the corresponding fluxes through the faces $e \in \Gamma_{ij}$ as

$$U_e^{k,m} = \mathbf{u}_h^{k,m}(e) \cdot \check{\mathbf{n}}(e). \tag{20}$$

We also retrieve the corresponding pressure at Γ_{ij} , but since for the RT_0 element the pressure nodes are located at the center of the computational cells, face pressure values must be recovered by using Darcy’s law. This amounts to compute a face pressure at each fine grid cell that intersects the boundary $\Gamma_{i,j}$. For instance, for an east boundary and fine grid cell I, J (see Fig. 1), we obtain the face pressure $\pi_h^{k,m}(e)$ by solving

$$U_e^{k,m} = -K_{I,J} \frac{\pi_h^{k,m}(e) - p_{h,I,J}^{k,m}}{h/2}. \tag{21}$$

In this way we end up, for each $\Gamma_{i,j}$, for each $k = i$ or j , and for each $m = 1, \dots, N_k$, with two column arrays $\tilde{U}^{k,m}$ and $\tilde{P}^{k,m}$, each of dimension M_{ij} (the number of fine grid faces in $\Gamma_{i,j}$), whose components are $U_e^{k,m}$ and $\pi_h^{k,m}(e)$, respectively. We define new column arrays denoted by $\underline{U}^{k,m}$ and $\underline{P}^{k,m}$ by subtracting the constant component of $\tilde{U}^{k,m}$ and $\tilde{P}^{k,m}$ which are finally used to build the snapshot matrices

$$\begin{aligned} \mathbb{A}_U^{\Gamma_{ij}} &= [\underline{U}^{i,1}, \dots, \underline{U}^{i,N_i}, \underline{U}^{j,1}, \dots, \underline{U}^{j,N_j}] \\ \mathbb{A}_P^{\Gamma_{ij}} &= [\underline{P}^{i,1}, \dots, \underline{P}^{i,N_i}, \underline{P}^{j,1}, \dots, \underline{P}^{j,N_j}] \end{aligned}$$

The next step is to perform the SVD decomposition on the two matrices above. The SVD decomposition of a given matrix $\mathbb{A} \in \mathbb{R}^{m \times n}$ reads

$$\mathbb{A} = \mathbb{X} \Sigma \mathbb{Y}^T$$

where $\mathbb{X} \in \mathbb{R}^{m \times m}$ and $\mathbb{Y} \in \mathbb{R}^{n \times n}$ are orthogonal matrices and $\Sigma \in \mathbb{R}^{m \times n}$ is a diagonal matrix given by

$$\Sigma = \text{diag}(\sigma_1, \dots, \sigma_q, 0, \dots, 0) \tag{22}$$

where $\sigma_1 \geq \sigma_2 \geq \dots \geq \sigma_q > 0$ are the singular values of the decomposition and q is the rank of matrix \mathbb{A} . This procedure is executed on both $\mathbb{A}_U^{\Gamma_{ij}}$ and $\mathbb{A}_P^{\Gamma_{ij}}$.

Finally, the informed space $\mathcal{U}_H^{\text{inf},k}$ (respectively, $\mathcal{P}_H^{\text{inf},k}$) is defined locally on each $\Gamma_{i,j}$ as the space of linear combinations of the first $k - 1$ right singular vectors of $\mathbb{A}_U^{\Gamma_{ij}}$ (respectively, $\mathbb{A}_P^{\Gamma_{ij}}$) augmented with the constant function on the corresponding interface.

Two comments are in order for the procedure just described. First, the number of local problems of type (16) to be solved can be reduced significantly by adopting a different strategy to parameterize the solution, for instance, by grouping together several fine grid faces on $\partial\omega$ on which some specified boundary conditions can be applied. Also randomly sampling these fine grid faces is a possibility [6]. Second, in the proposed approach, the solutions of the local problems are considered all equally probable prior to computing the SVD decomposition. However, some strategy could be devised to discard solutions of small norm on the interface. These topics will be the subject of future studies.

4. Numerical experiments

We have performed a series of numerical experiments in a quarter of a 5-spot geometry in a rectangular 2D region with dimensions $[0, 11/3] \times [0, 1]$. We consider no-flow boundary conditions with an injection (production) well positioned at the top left (bottom right) corner of the computational region. For the absolute permeability we take

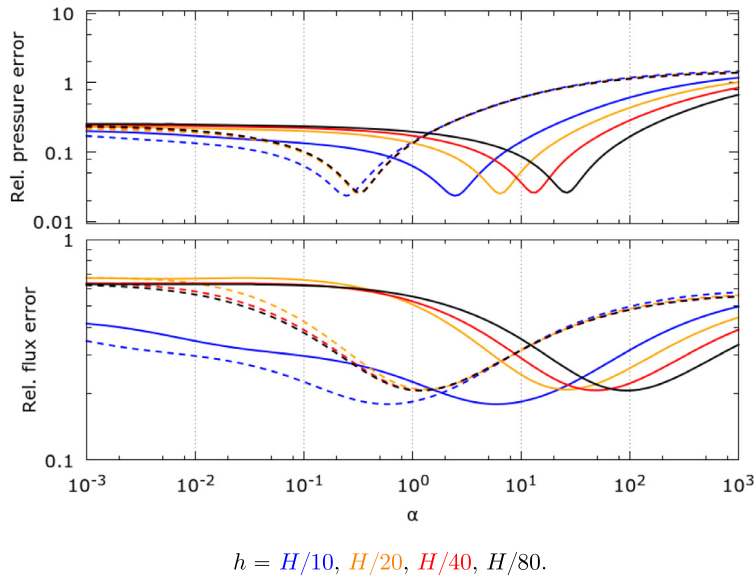


Fig. 2. Effect on α position for $L = h$ (solid lines) and $L = H$ (dashed lines) for a sequence of fine mesh refinement.

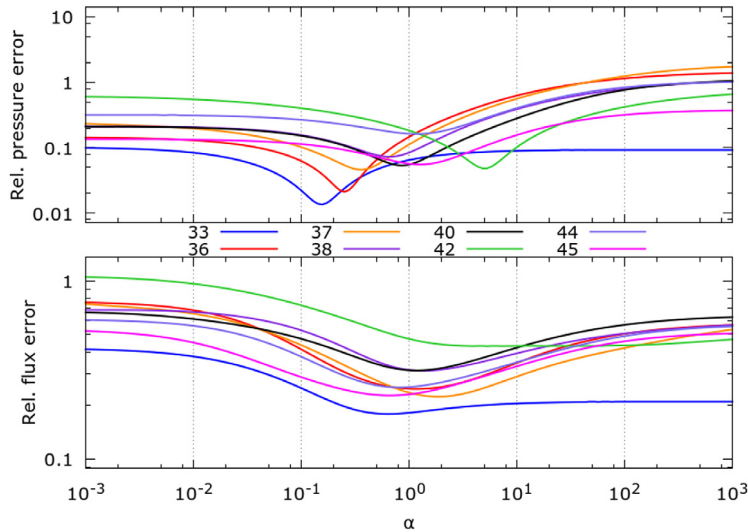


Fig. 3. Relative pressure errors (top) and relative flux errors (bottom) for a collection of SPE10 layers with $L = H$.

distinct layers of the SPE10 project (<http://www.spe.org/web/csp>) [7]. These are realistic, very heterogeneous fields typical of petroleum reservoirs.

The interface spaces are either polynomials or informed spaces obtained with oversampling of size h . We consider the flux boundary operator given by Eq. (18) and the average pressure is set to zero. The results are given in the form of graphs that display the relative $L^2(\Omega)$ error norm (computed with respect to the fine grid solution) for the pressure and flux variables. We first investigate the adequate characteristic length scale for the nondimensionalization of the numerical parameter β , and then explore the accuracy of the MRCM compared with the MMMFEM and the MHM with same number of interface unknowns. Finally, we perform an exhaustive comparison study covering all the SPE10 layers.

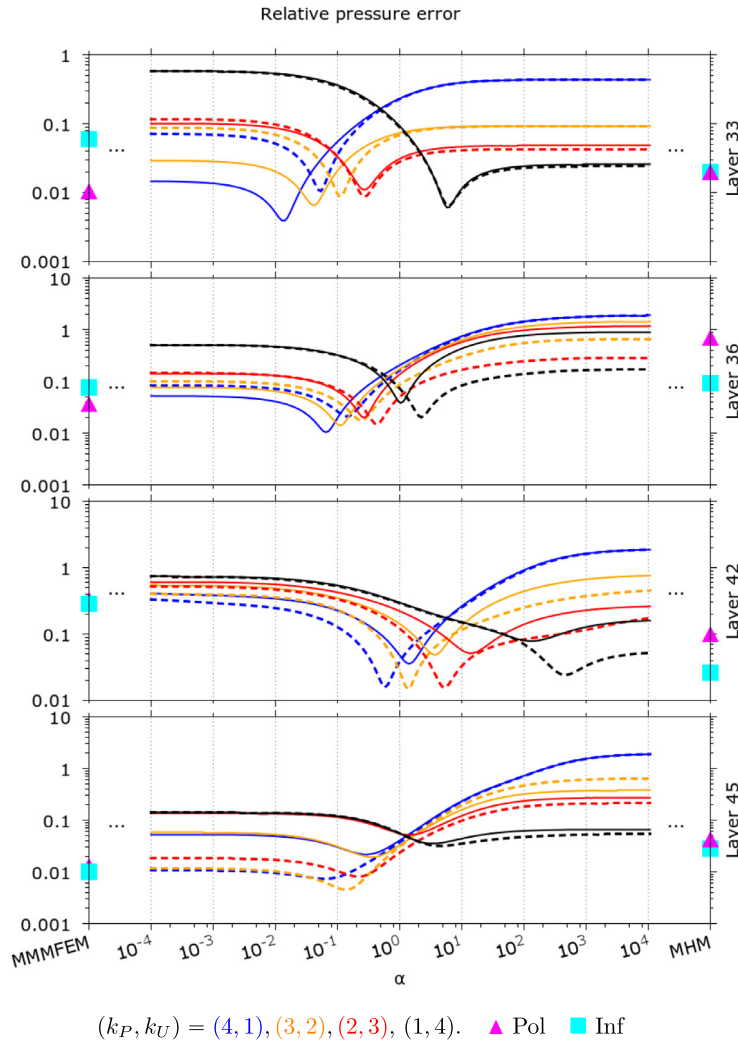


Fig. 4. Relative pressure error as function of α for layers 33, 36, 42 and 45 with 5 dof's. Solid lines: polynomial spaces; Dashed lines: informed spaces, for the MRCM formulation.

4.1. The characteristic length scale

Dimensional analysis indicates that the Robin coefficient of subdomain i can be written in terms of a dimensionless α as

$$\beta_i(\mathbf{x}) = \frac{\alpha(\mathbf{x})L}{K(\mathbf{x})}.$$

In [15], we set $L = h$, h being the mesh size. Here we show that a better choice is $L = H$, where H is the size of $\Gamma_{ij} = \partial\Omega_i \cap \partial\Omega_j$. To see this we fix the decomposition of the computational region and perform a mesh refinement study inside subdomains. Although α could in general depend on \mathbf{x} , we adopt a fixed value for it that holds for all \mathbf{x} and all i . For the choice $L = H$ the value of α for which the MRCM yields minimum error remains essentially unaltered under the refinement study. In order to illustrate our findings, we consider layer 36 (that contains a high contrast channel) divided into 22×6 rectangular subdomains with size $H \times H$, being $H = 1/6$. For this domain decomposition we consider a sequence of mesh refinements inside each subdomain starting with 10×10 (mesh size $h = H/10$) and increase each direction by a factor of 2 until we reach $h = H/80$. For the interface spaces we consider here polynomials of degree one, i.e., $\mathcal{U}_H = \mathcal{U}_H^{\text{pol},2}$ and $\mathcal{P}_H = \mathcal{P}_H^{\text{pol},2}$.

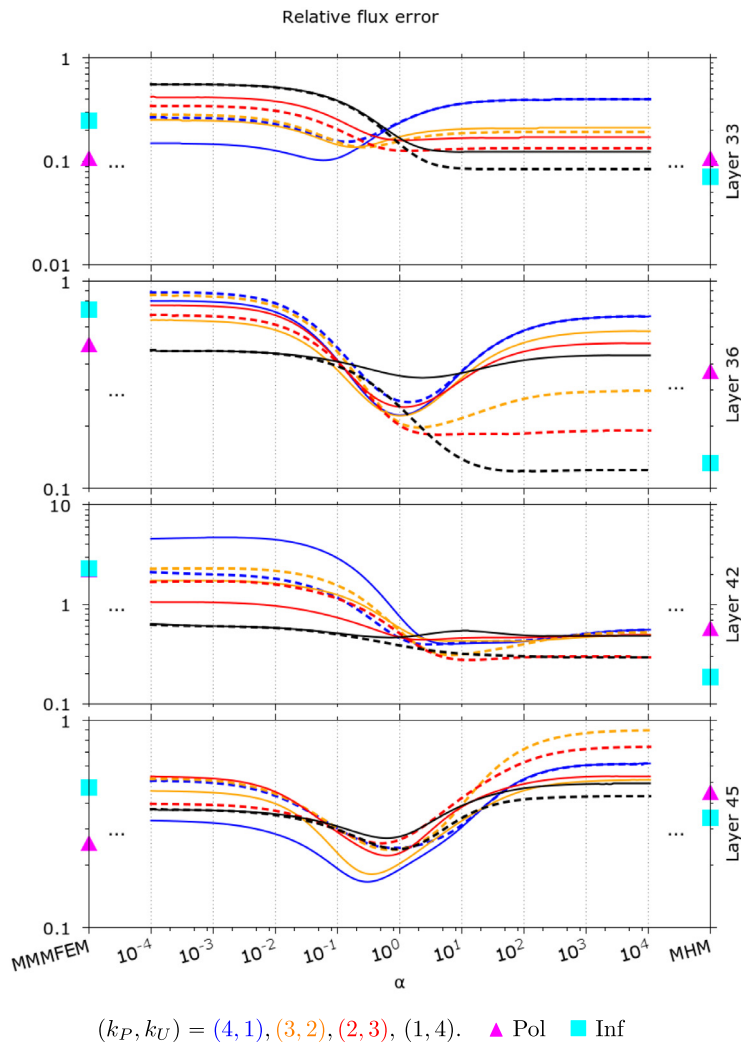


Fig. 5. Relative flux error as function of α for layers 33, 36, 42 and 45 with 5 dof's. Solid lines: polynomial spaces; Dashed lines: informed spaces, for the MRCM formulation.

As can be seen in Fig. 2, where we report the errors against the parameter α , if one sets $L = h$ (solid lines) the optimal value for α increases for both pressure and fluxes as the mesh is refined. On the other hand, if one sets $L = H$ (dashed lines) the value of α for which the error is minimal turns out to be quite independent of h , with $\alpha \sim 0.3$ to minimize pressure error and $\alpha \sim 1$ to minimize flux error. This suggests that one could simply assign a fixed value to α .

To further confirm this, we solve the same problem with another decomposition given by 11×3 subdomains ($H = 1/3$) and a fixed mesh of 20×20 elements per subdomain (i.e., $h = H/20$). Further, we consider several permeability fields taken from different layers of the SPE10 data. As before, the interface spaces are $\mathcal{U}_H^{\text{pol},2}$ and $\mathcal{P}_H^{\text{pol},2}$ (piecewise linear polynomials). In Fig. 3 we illustrate the relative errors for pressure and flux as functions of α . Note that the minimum error remains close to $\alpha = 1$, especially for the flux error, in all cases.

Given the results reported above, from now on we adopt $L = H$ in the definition of the Robin parameter.

4.2. Comparison of multiscale mixed methods

Here we focus on numerical solutions computed with the MRCM, in comparison to those provided by the MMMFEM and the MHM. Through numerical simulations we have shown (see [15]) that as $\alpha \rightarrow +0$ the flux

Layer 36 pressure solution

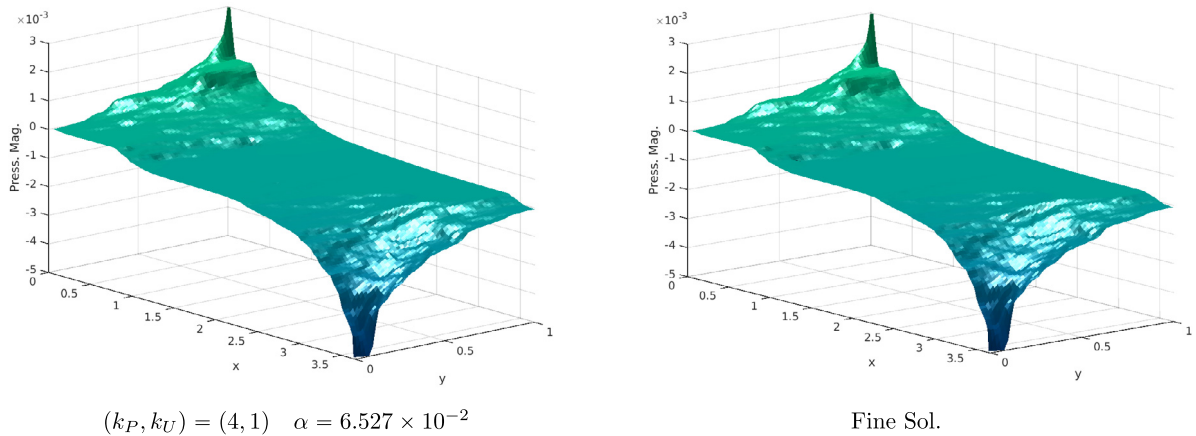


Fig. 6. Pressure solution for the optimal global α and interface spaces with 5 *dof*'s for polynomials and the fine pressure solution for layer 36.

interface space \mathcal{U}_H becomes irrelevant and the MRCM produces results that tend to those of the MMMFEM with the interface space \mathcal{P}_H . On the other hand, as $\alpha \rightarrow +\infty$, \mathcal{P}_H becomes irrelevant and the MRCM produces results that tend to those computed with the MHM with the interface space \mathcal{U}_H . In conclusion, one can view the MRCM as a generalization of the two other known procedures.

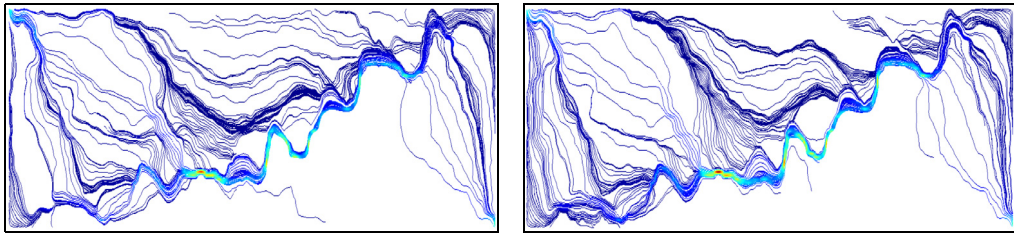
The comparison among the three methodologies will be conducted as follows: For each numerical study we fix a number k of degrees of freedom (*dof*'s) per interface $\Gamma_{i,j}$ to be employed in solutions computed with all methods. For the MMMFEM we set $\mathcal{P}_H = \mathcal{P}_H^{\text{pol},k}$ in the case of piecewise polynomial spaces, and $\mathcal{P}_H = \mathcal{P}_H^{\text{inf},k}$ in the case of informed spaces. Similarly, for the MHM we set \mathcal{U}_H equal to either $\mathcal{U}_H^{\text{pol},k}$ or $\mathcal{U}_H^{\text{inf},k}$. For the MRCM we take the interface spaces to be $\mathcal{P}_H^{\text{pol},k_P}$ (or $\mathcal{P}_H^{\text{inf},k_P}$ in the informed case) and $\mathcal{U}_H^{\text{pol},k_U}$ (or $\mathcal{U}_H^{\text{inf},k_U}$), with $k_U + k_P = k$.

Initially we set $k = 5$ *dof*'s per interface and take some representative layers of the SPE10 database. We select layer 33 that does not exhibit a strong channelized structure, layer 36 with one well defined channel, and layers 42 and 45 with an intricate channel structure. In our studies we set $K_{\max}/K_{\min} \simeq 10^6$. In Figs. 4 and 5 we display the relative $L^2(\Omega)$ error norms for pressure and flux variables, respectively, as functions of α . When comparing the MRCM pressure with that of the MMMFEM (left dots) and that of the MHM (right dots) it is clear that one can always find a combination of (k_P, k_U) and α such that the MRCM produces a more accurate result than MMMFEM and MHM for both polynomial (solid lines) and informed (dashed lines) interface spaces. This observation is valid except for layer 45, for which the MMMFEM solution for the polynomial space is superior. This conclusion remains the same when comparing the flux errors. Exceptions to this finding occur on layers 33 and 42, for which the MHM produces the most accurate results for the case of informed spaces. In order to exhibit the quality of the solution, Figs. 6 and 7 display the pressure solution and the streamlines for the best global α compared to the fine solution for layer 36 for the polynomial case. In Figs. 8 and 9 we illustrate the relative $L^2(\Omega)$ error norms for pressure and flux variables, respectively, as a function of α for the case of $k = 4$ with layers 30, 63, 67 and 75, which were selected using the same criterion as adopted above, although none of the fields with channelized structure (layers ≥ 63) present one well-defined channel as in layer 36. In the numerical studies just discussed, that focus on global errors, we have shown that one can often find a combination of k_P, k_U and α for the MRCM that produces a better numerical solution than that provided by MMMFEM and MHM.

Next, we investigate how the error is distributed aiming at assessing the importance of informed spaces in approximating the velocity field in high-contrast realistic channelized formations. We take the permeability field with the most pronounced channel (layer 36), $k = 5$, and the best combination of (k_P, k_U) and α for polynomial and informed spaces that minimize the corresponding global error, as depicted on Figs. 4 and 5.

In Figs. 10 and 11 we show the pointwise absolute errors for pressure and flux, respectively. From these results one can see that both strategies provide comparable approximations for the pressure field (see Fig. 10). However, Fig. 11

Layer 36 streamlines



$(k_P, k_U) = (3, 2) \quad \alpha = 1.035 \times 10^0$

Fine Sol.

Fig. 7. Streamlines for the optimal global α and interface spaces with 5 dof's for polynomials and the fine solution for layer 36.

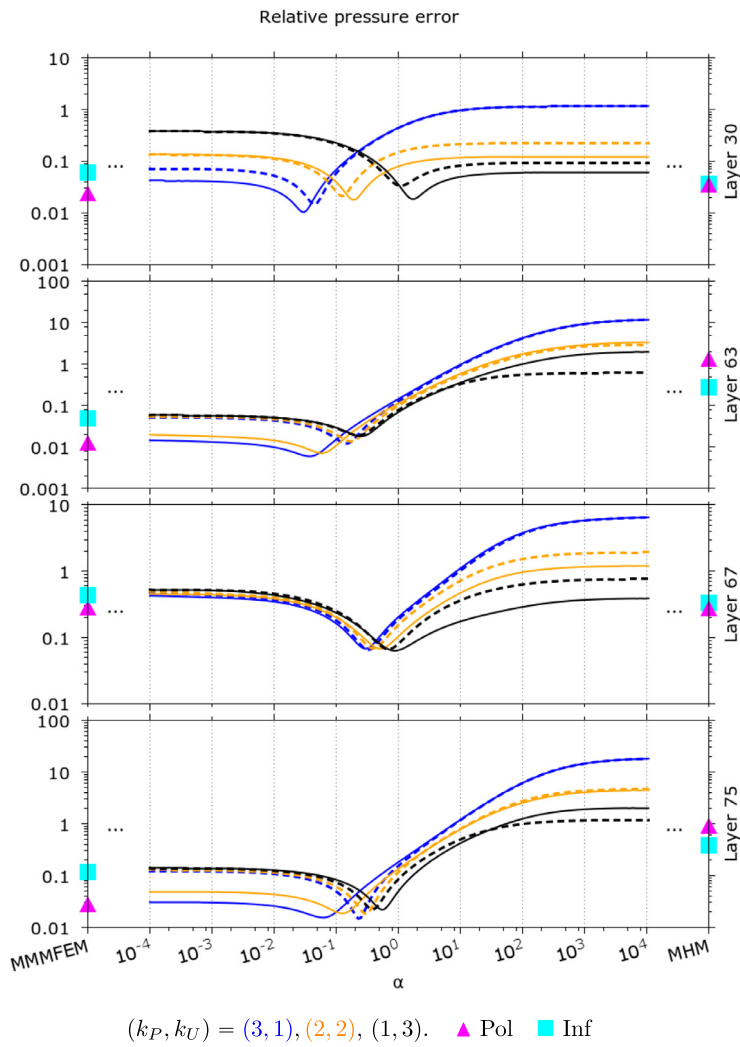


Fig. 8. Relative pressure error as function of α for layers 30, 63, 67 and 75 with 4 dof's. Solid lines: polynomial spaces; Dashed lines: informed spaces, for the MRCM formulation.

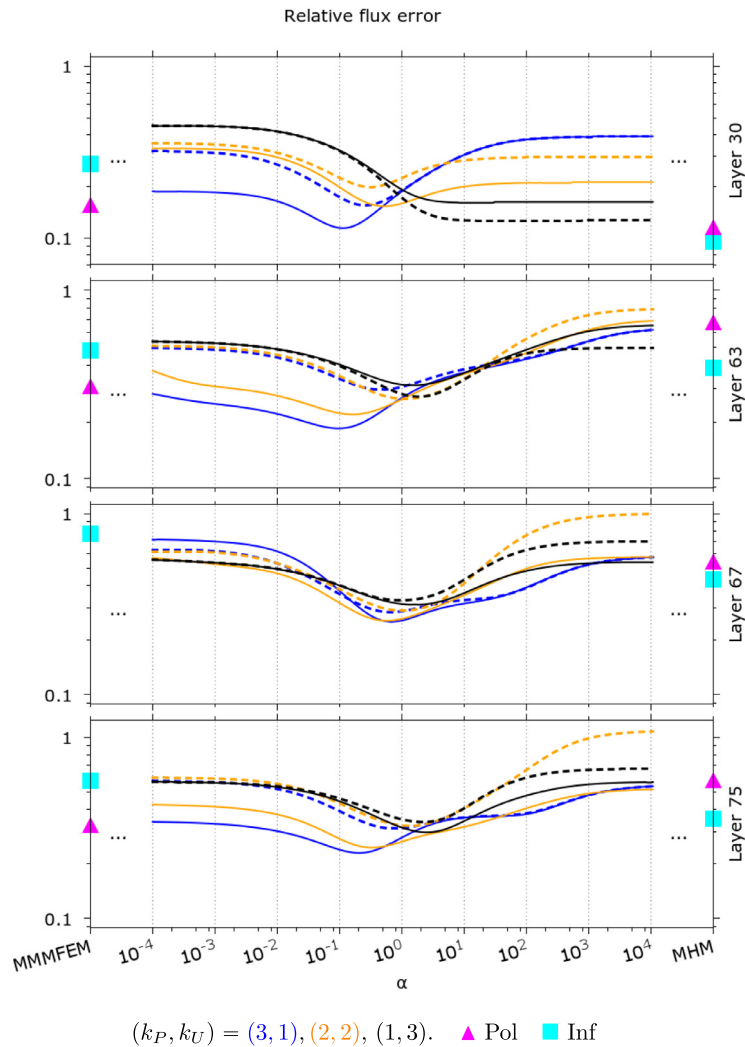


Fig. 9. Relative flux error as function of α for layers 30, 63, 67 and 75 with 4 *dof*'s. Solid lines: polynomial spaces; Dashed lines: informed spaces, for the MRCM formulation.

indicates that informed spaces produce a better approximation of the flux variable than its polynomial counterpart. Moreover, the error is larger on the main channel structure of the permeability field for the polynomial compared to the informed case. Thus, informed spaces show great potential to be applied in reservoir simulation.

The studies discussed above illustrate that the accuracy of results produced by the MRCM depend on the choice of (k_P, k_U) and α . They also confirm, as noted by Guiraldello et al. [15], that intermediate values of α are “safe”, in the sense that they lead to errors that are *never* larger, and usually smaller, than the errors produced by the extreme values $\alpha = 0$ (MMMFEM) and $\alpha = +\infty$ (MHM). In order to avoid the need of selecting (k_P, k_U) and α at each run of the MRCM, we adopt the following strategy that has worked well in numerous tests:

- If k is even, we take $k_P = k_U = k/2$;
- if k is odd, we take $k_P = (k - 1)/2$ and $k_U = k_P + 1 = k - k_P$;
- set $\alpha = 1$.

In this way there are no free parameters for the MRCM. To justify such choices we perform an exhaustive comparison of MRCM, MHM and MMMFEM, with the same number k of *dof*'s per interface for all methods, considering all SPE10 layers. Both polynomial and informed spaces are considered and the three methods can be compared on an

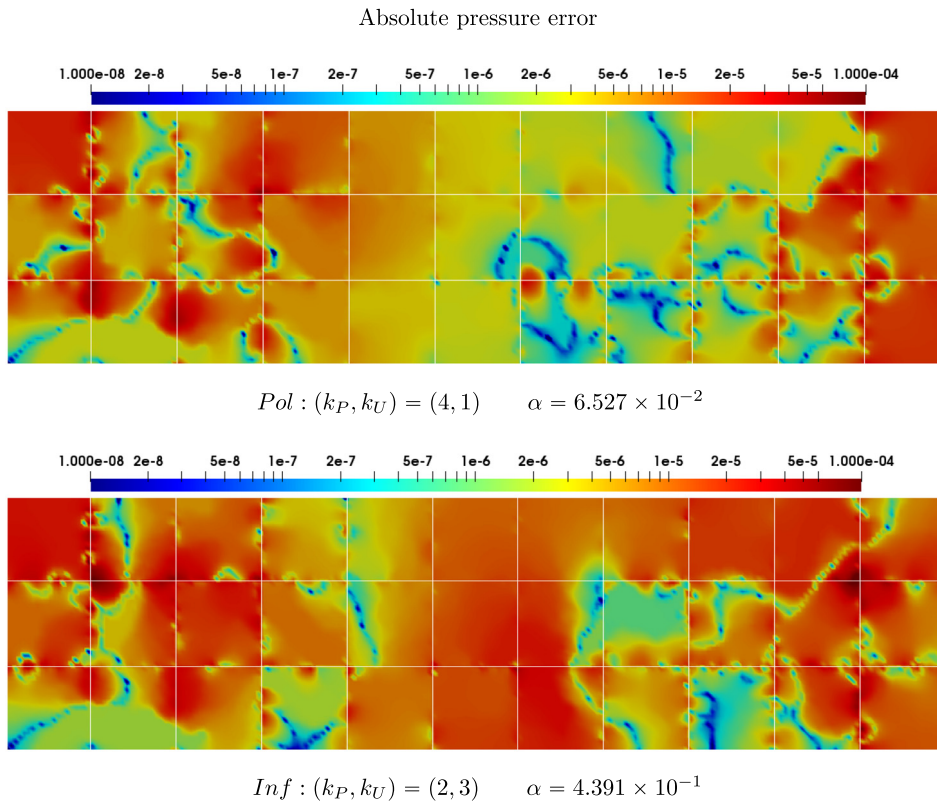


Fig. 10. Absolute pressure error for the optimal global α and interface spaces with 5 *dof*'s for polynomial and informed interface spaces for layer 36.

equal footing. Figs. 12 and 14 show, respectively, the results for $k = 4$ and $k = 5$ for polynomial interface spaces. Note that when a curve corresponding to any of the methods appears in the shadowed region of another curve with a larger error, the color gets darker. For this choice of parameters the MHM is the least accurate method in the pressure variable for the channelized layers (layer number > 35), the MMMFEM being the most accurate. For the flux variable, however, the most accurate is the MRCM, while the MMMFEM behaves quite poorly for some of the layers around layer 40. The corresponding study for informed spaces is given in Figs. 13 and 15. For these spaces the MHM is again the least accurate procedure in the pressure variable (especially in layers 65–75), while the MMMFEM and MRCM behave similarly. For the flux variable the MHM and MRCM yield similar accuracy, better than that of the MMMFEM, which again is considerably worse than the others for the layers around layer 40.

Although the focus of previous experiments is accuracy, another equally important aspect is the efficiency of the numerical methods. In order to illustrate this aspect, Fig. 16 displays the number of GMRES iterations to convergence to solve the interface problem for each method with $k = 5$ for all the SPE10 layers with polynomial functions for the MMMFEM and MRCM and informed functions for the MHM. The GMRES was set with a relative tolerance of 10^{-9} and an ILU preconditioner with a drop tolerance of 10^{-4} . From the results one can observe that the MMMFEM and the MRCM have comparable number of GMRES iterations, with a slight advantage for the MRCM, and converge with half of the iterations required for the MHM. In these experiments the linear systems being solved have 260 unknowns. Another important point is that all of the above experiments are based on a fixed domain decomposition of 11×3 subdomains. In order to explore other configurations, Fig. 17 displays the relative error to convergence for many different domain decomposition geometries with $k = 5$ for layer 36. Notice that, as the global fine mesh is fixed and each subdomain is a collection of fine elements, the number of elements for each domain decomposition geometry are different, e.g., each subdomain of the 5×6 domain decomposition geometry has a fine mesh of 44×10 elements.

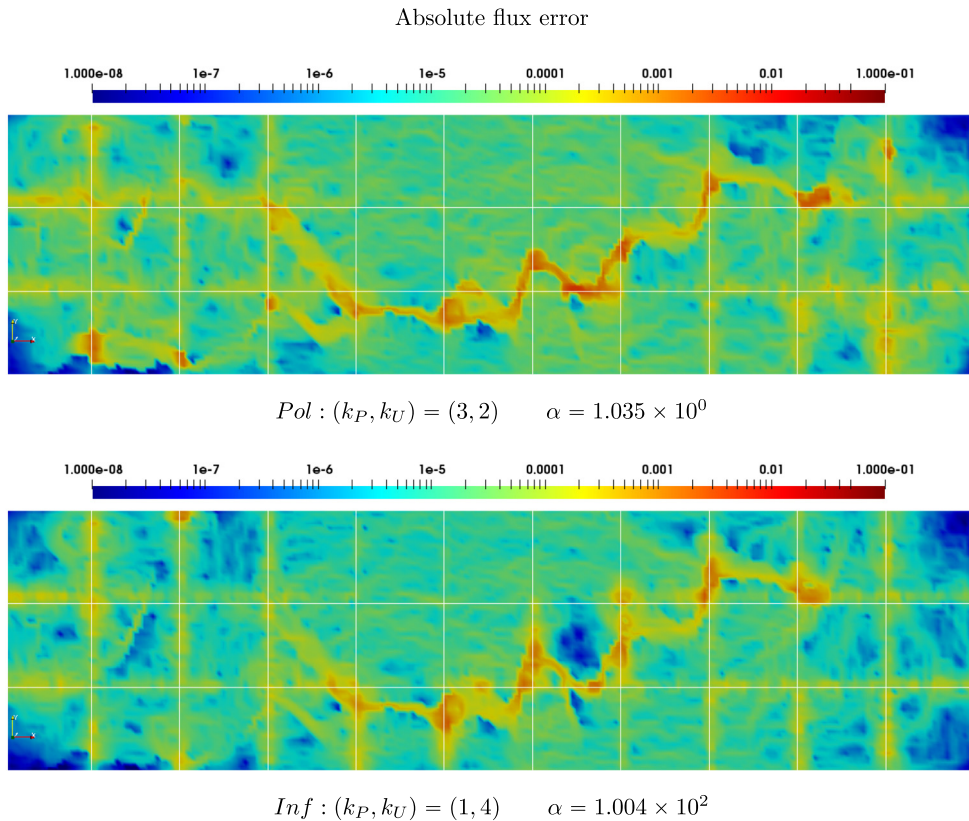


Fig. 11. Absolute flux error for the optimal global α and interface spaces with 5 *dof*'s for polynomial and informed interface spaces for layer 36.

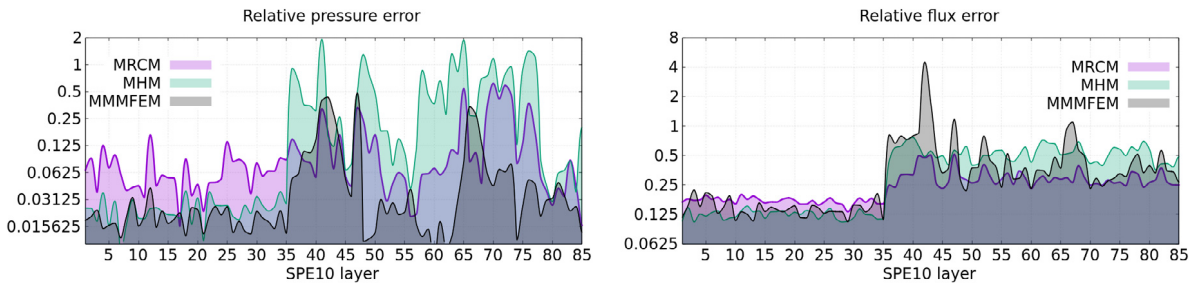


Fig. 12. Relative pressure and flux error for all the SPE10 layers considering $k = 4$ and polynomial functions to build the interface spaces.

The results shown in Figs. 12–17 allow us to conclude that the proposed MRCM is a competitive alternative to MMMFEM and MHM, both with polynomial and informed interface spaces. It should however be noted that the error obtained with informed spaces is roughly the same as that obtained with polynomial spaces. The only salient effect is the reduction of the pressure error, and just for the MHM.

Overall, the numerical results reported here indicate that the MRCM, with suitable choices for the spaces and parameters, is able to produce more accurate solutions than the other two procedures for problems defined for realistic, very heterogeneous permeability fields.

5. Concluding remarks

We have reviewed the recently introduced Multiscale Robin Coupled Method and described its implementation with informed spaces (or empirical interpolation spaces, obtained by oversampling) for the interface variables. We

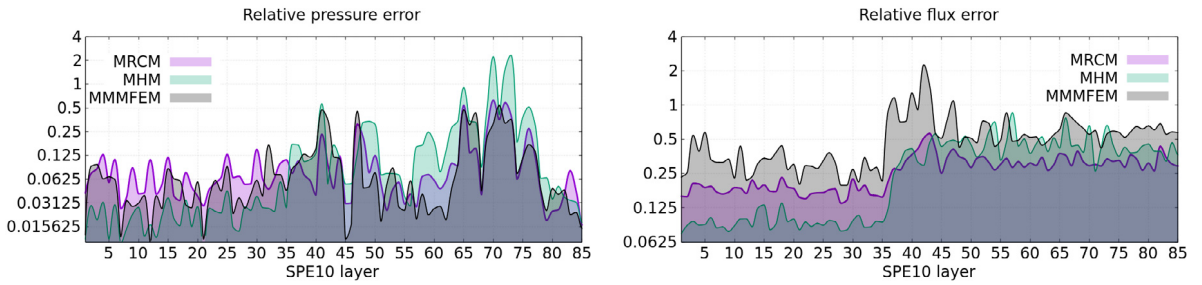


Fig. 13. Relative pressure and flux error for all the SPE10 layers considering $k = 4$ and informed functions to build the interface spaces.

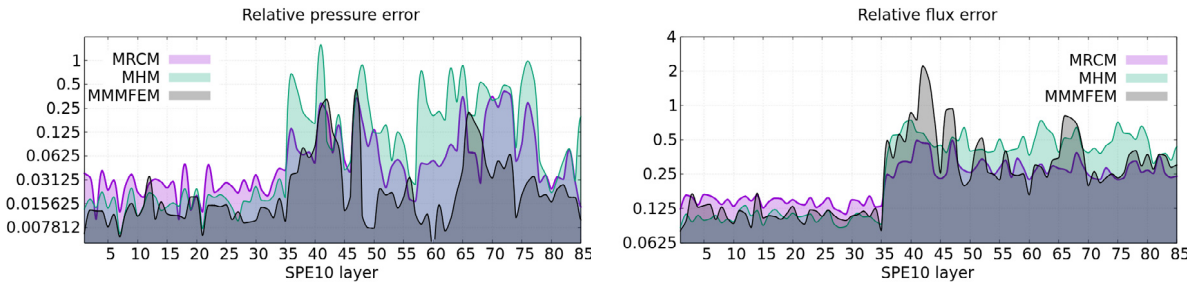


Fig. 14. Relative pressure and flux error for all the SPE10 layers considering $k = 5$ and polynomial functions to build the interface spaces.

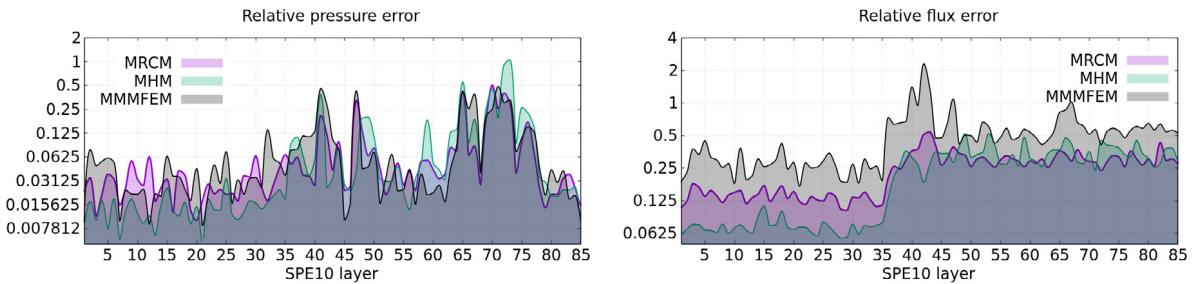


Fig. 15. Relative pressure and flux error for all the SPE10 layers considering $k = 5$ and informed functions to build the interface spaces.

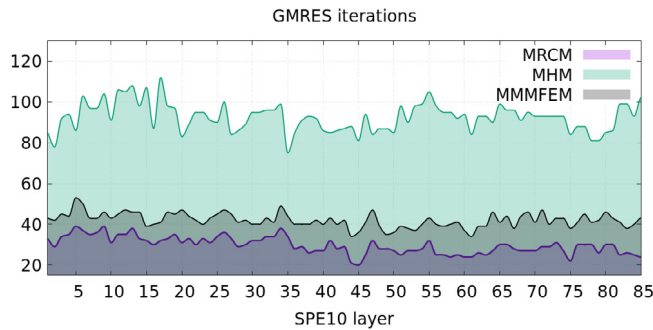


Fig. 16. Number of GMRES iterations to convergence for all the SPE10 layers with $k = 5$.

have compared the accuracy of the solutions of two well known multiscale methods, the Multiscale Mortar Mixed Finite Element Method and the Mixed Hybrid Method, with that of the MRCM in realistic, very heterogeneous permeability fields given by layers of the SPE10 project. The comparison was carried out with the same number of

Domain decomposition geometries

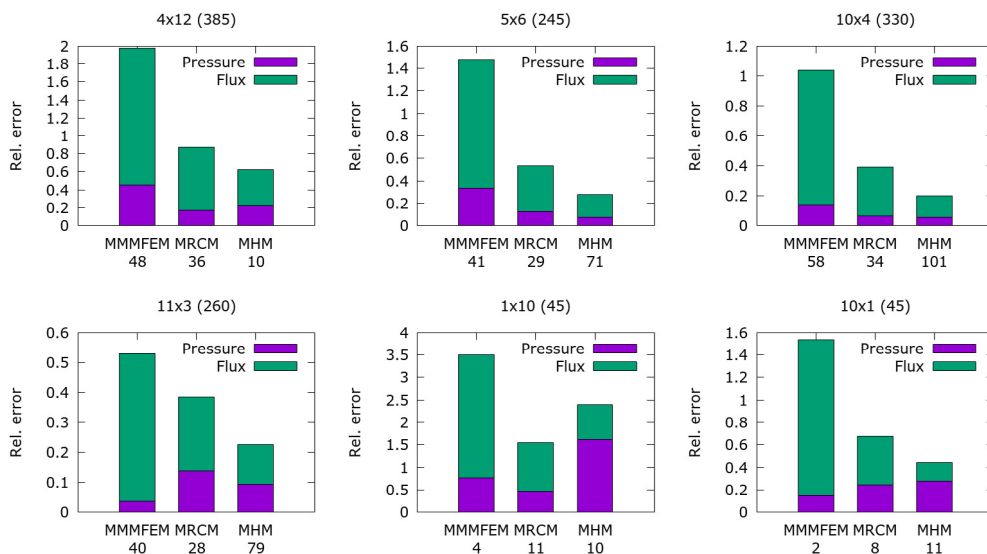


Fig. 17. Relative pressure and flux errors and number of GMRES iterations, indicated below the labels, to convergence for different domain decomposition geometries indicated at top of each graph with the number of unknowns being solved in parenthesis, for the layer 36 with $k = 5$.

unknowns for all methods, with interface spaces given by polynomial and informed functions. It should be mentioned that no such comparison is available even if restricted to MMMFEM and MHM, and that no previous implementation or assessment of the MHM with informed spaces has been reported in the literature.

Our numerical results indicate that the MRCM, fixing its algorithmic parameter α to the value 1 and with a balanced distribution of the unknowns between interface pressures and interface fluxes, is a competitive alternative to the two previous methods. In fact, it is more accurate than MHM (which behaves better than MMMFEM) for the flux variable in highly channelized cases, without the large pressure errors produced by MHM.

Further work is needed to establish new, effective strategies for the construction of informed spaces. The simple procedures explored in this work have been useful for studying the optimal distribution of unknowns between interface pressures and fluxes, but the reduction in the solution global error was not significant, although it shows improved local approximations for the fluxes in channelized formations. Moreover, it was also shown that the MHM, when the interface spaces are switched from polynomial to informed (with the specific spaces proposed), exhibits essentially the same flux error but with a noticeable decrease of the pressure error. The identification of informed spaces with similar positive effects on the MRCM are left for future studies.

Acknowledgments

The authors gratefully acknowledge the financial support received from the São Paulo Research Foundation FAPESP, grant 2013/07375-0 CEPID/CeMEAI, grant 2016/08115-0 and grant 2015/02649-0; from the Brazilian National Research and Technology Council (CNPq), Science Without Borders grant 400169/2014-2; and from Brazilian Petroleum Corporation (Petrobras). FP was also funded in part by National Science Foundation (NSF), grant DMS 1514808, and by The University of Texas at Dallas.

References

- [1] R. Araya, C. Harder, D. Paredes, F. Valentin, Multiscale hybrid-mixed method, *SIAM J. Numer. Anal.* 51 (6) (2013) 3505–3531.
- [2] T. Arbogast, G. Pencheva, M.F. Wheeler, I. Yotov, A multiscale mortar mixed finite element method, *SIAM Multiscale Model. Simul.* 6 (1) (2007) 319–346.
- [3] I. Babuska, E. Osborn, Generalized finite element methods: their performance and their relation to mixed methods, *SIAM J. Numer. Anal.* 31 (1983) 510–536.

- [4] S. Bosma, H. Hajibeygi, M. Tene, H.A. Tchelepi, Multiscale finite volume method for discrete fracture modeling on unstructured grids (MS-DFM), *J. Comput. Phys.* 351 (2017) 145–164.
- [5] V.M. Calo, Y. Efendiev, J. Galvis, M. Ghommem, Multiscale empirical interpolation for solving nonlinear pdes using generalized multiscale finite element methods, 2014, arXiv preprint arXiv:1407.0103v1.
- [6] V.M. Calo, Y. Efendiev, J. Galvis, G. Li, Randomized oversampling for generalized multiscale finite element methods, *SIAM Multiscale Model. Simul.* 14 (1) (2016) 482–501.
- [7] M. Christie, M. Blunt, Tenth SPE comparative solution project: A comparison of upscaling techniques, in: SPE-66599-MS, Society of Petroleum Engineers, 2001.
- [8] E.T. Chung, Y. Efendiev, T. Hou, Adaptive multiscale model reduction with generalized multiscale finite element methods, *J. Comput. Phys.* 320 (2016) 69–95.
- [9] E.T. Chung, Y. Efendiev, W.T. Leung, Fast online generalized multiscale finite element method using constraint energy minimization, *J. Comput. Phys.* 355 (2018) 450–463.
- [10] E.T. Chung, S. Fu, Y. Yang, An enriched multiscale mortar space for high contrast flow problems, 2016, arXiv preprint arXiv:1609.02610.
- [11] Compositional multiscale finite-volume formulation, *Soc. Petrol. Eng.* 19 (2).
- [12] J. Douglas, P.J. Paes-Leme, J.E. Roberts, J.P. Wang, A parallel iterative procedure applicable to the approximate solution of second order partial differential equations by mixed finite element methods, *Numer. Math.* 65 (1) (1993) 95–108.
- [13] A. Francisco, V. Ginting, F. Pereira, J. Rigelo, Design and implementation of a multiscale mixed method based on a nonoverlapping domain decomposition procedure, *Math. Comput. Simulation* 99 (2014) 125–138.
- [14] B. Ganis, I. Yotov, Implementation of a mortar mixed finite element method using a multiscale flux basis, *Comput. Methods Appl. Mech. Engrg.* 198 (2009) 3989–3998.
- [15] R.T. Guiraldello, R.F. Ausas, F.S. Sousa, F. Pereira, G.C. Buscaglia, The multiscale Robin coupled method for flows in porous media, *J. Comput. Phys.* 355 (2018) 1–21.
- [16] H. Hajibeygi, G. Bonfigli, M.A. Hesse, P. Jenny, Iterative multiscale finite-volume method, *J. Comput. Phys.* 227 (19) (2008) 8604–8621.
- [17] C. Harder, D. Paredes, F. Valentin, On a multiscale hybrid-mixed method for advective-reactive dominated problems with heterogeneous coefficients, *SIAM Multiscale Model. Simul.* 13 (2) (2015) 491–518.
- [18] P. Jenny, S.H. Lee, H.A. Tchelepi, Multi-scale finite-volume method for elliptic problems in subsurface flow simulation, *J. Comput. Phys.* 187 (2003) 47–67.
- [19] S.H. Lee, H. Zhou, H.A. Tchelepi, Adaptive multiscale finite-volume method for nonlinear multiphase transport in heterogeneous formations, *J. Comput. Phys.* 228 (24) (2009) 9036–9058.
- [20] I. Lunati, P. Jenny, Multiscale finite-volume method for compressible multiphase flow in porous media, *J. Comput. Phys.* 216 (2) (2006) 616–636.